Article

Discovery Medicine 2025; 37(198): 1359–1371
https://doi.org/10.24976/Discov.Med.202537198.118

Activation of TRPV4 Downregulates TGF-β1 Protein Levels to Promote M1 Polarization of BV-2 Microglia and Induce Apoptosis in HT22 Neuronal Cells

Ting Zhou[1,†], Ronggui Zhang[2,†], Chao Yang[1], Jianfang Wei[1], Ying Feng[1,*]

[1]Department of Neurology, People's Hospital of Dongxihu District, 430040 Wuhan, Hubei, China
[2]Department of Infectious Diseases, People's Hospital of Dongxihu District, 430040 Wuhan, Hubei, China
*Correspondence: fengying.5240@163.com (Ying Feng)
[†]These authors contributed equally.
Published: 20 July 2025

Background: The pathological hallmarks of Alzheimer's disease (AD) include microglial polarization toward the pro-inflammatory M1 phenotype and significant neuronal apoptosis. Overactivation of transient receptor potential vanilloid 4 (TRPV4) channels has been identified as a common feature in AD animal models associated with microglial activation and neuronal injury. However, the downstream molecules and signaling pathways regulated by TRPV4 remain incompletely understood. Therefore, this study aimed to elucidate the mechanisms by which TRPV4 promotes microglial M1 polarization and its subsequent effect on hippocampal neuronal apoptosis.

Methods: BV-2 cells were employed as an *in vitro* model to mimic microglial function, while HT22 cells represented hippocampal neurons. BV-2 cells were treated with the TRPV4 activator GSK1016790A, the TRPV4 antagonist HC-067047, and exogenous recombinant human transforming growth factor-beta 1 (TGF-β1) protein. Following treatment, phagocytic activity was evaluated by co-culturing BV-2 cells with fluorescent microspheres. Enzyme-linked immunosorbent assay was performed to quantify cytokine levels in the supernatant. The proportion of M1 phenotype cells was determined by immunofluorescence staining. Additionally, TGF-β1 protein expression and NF-κB pathway activation were evaluated via Western blot analysis. Subsequently, supernatants from BV-2 cells were collected as a conditioned medium to culture HT22 cells. Cell viability of HT22 cells was assessed using the MTT assay, and apoptosis was measured via Terminal deoxynucleotidyl transferase dUTP nick end labeling (TUNEL) staining.

Results: TRPV4 activation significantly enhanced the phagocytic activity and pro-inflammatory cytokine release in BV-2 cells, elevated M1 phenotype marker expression, reduced intracellular TGF-β1 protein levels, and activated the NF-κB signaling pathway ($p < 0.05$). Additionally, TRPV4 activation impaired HT22 cell viability and significantly promoted apoptosis ($p < 0.01$). However, treatment with HC-067047 or exogenous TGF-β1 partially reversed the adverse effects of TRPV4 activation on BV-2 and HT22 cells.

Conclusion: *In vitro* models demonstrated that TRPV4 activation downregulates TGF-β1 expression and activates the NF-κB signaling pathway, thereby enhancing BV-2 microglial polarization toward the M1 phenotype and accelerating neuronal apoptosis. These findings provide a theoretical foundation for developing novel AD therapies targeting TGF-β1, highlighting its potential clinical significance.

Keywords: Alzheimer's disease; TRPV4; microglial polarization; TGF-β1

Introduction

As the most prevalent form of neurodegenerative disease, Alzheimer's disease (AD) is characterized by memory impairment, cognitive decline, and psychiatric symptoms [1]. With the global population ageing, the incidence and prevalence of AD are rising [2]. Data from the United States indicate that over 6.7 million Americans currently suffer from AD, a figure projected to reach 13.8 million by 2060 [3]. AD not only affects a vast number of individuals but also imposes considerable medical and caregiving costs, resulting in a significant global economic burden. In 2015, the global economic cost of AD exceeded $1 trillion, and this figure is projected to rise to $9.12 trillion by 2050 [4]. These findings suggest that AD has emerged as a significant global public health concern, reinforcing the urgency of clarifying its pathogenesis and developing clinically effective therapeutic strategies.

The pathological mechanisms of AD are complex and multifactorial, encompassing β-amyloid (Aβ) accumulation, neurofibrillary tangle (NFT) formation, mitochondrial dysfunction, and chronic neuroinflammation [5]. However,

extensive neuronal apoptosis in the hippocampus serves as the common downstream event triggered by these pathological processes and represents a central mechanism underlying the clinical manifestations of AD [6]. The hippocampus is recognized as a critical brain region responsible for memory and learning. Neuronal apoptosis in this region results in a marked reduction in neuronal numbers and disruption of neural networks. When the surviving neurons are insufficient to support higher-order neural activities, AD patients typically present with learning deficits and memory loss [7,8]. Therefore, mitigating neuronal apoptosis to preserve hippocampal neurons is a key strategy for delaying AD progression.

Microglia are the principal immune cells within the central nervous system (CNS). These cells originate either from neuroepithelial progenitors of the neuroectoderm or from peripheral mononuclear cells that migrate across the blood-brain barrier into the CNS. Microglia are abundant and widely distributed, comprising approximately 10–15% of total brain cells [9]. During AD progression, microglia play multifaceted roles [10]. In their anti-inflammatory phenotype (M2), microglia help clear pathological metabolites such as β-amyloid (Aβ) plaques and phosphorylated tau proteins, thereby maintaining CNS homeostasis and inhibiting disease progression [11]. However, under conditions of chronic neuroinflammation, microglia often polarize from the M2 to the pro-inflammatory M1 phenotype, secreting elevated levels of inflammatory cytokines that exacerbate neuronal damage and dysfunction, ultimately leading to significant neuronal apoptosis [12]. In this context, microglial activation accelerates AD progression. Thus, preventing the neuroinflammation-induced polarization of microglia toward the M1 phenotype may help reduce neuronal apoptosis, supporting its potential as a therapeutic target in AD management.

Transient receptor potential vanilloid 4 (TRPV4) is a non-selective cation channel highly sensitive to various exogenous stimuli, including mechanical stress, osmotic changes, and temperature fluctuations. These stimuli activate TRPV4, inducing calcium influx and significantly increasing intracellular calcium levels. TRPV4 is widely expressed across multiple organs and tissues and is particularly enriched in the CNS. In the brain, TRPV4 is notably distributed in regions such as the frontal cortex, hippocampus, thalamus, and cerebellum and is expressed in neurons, microglia, and astrocytes [13]. Research indicates that mechanical and chemical stimuli can activate TRPV4 on microglial membranes, leading to increased calcium influx, alterations in microglial morphology, and changes in intracellular signaling, which ultimately polarize microglia toward the M1 phenotype [14].

While most evidence on TRPV4 overactivation in AD arises from animal models, evidence from human studies supports its pathological relevance. For example, Bai and Lipski [15] showed that TRPV4 contributes to Aβ (40)-induced calcium dysregulation and neuronal apoptosis in human hippocampal slices, suggesting its abnormal activity in the human AD brain. Additionally, Zhang *et al.* [16] reported enhanced TRPV4 expression in the cortex and hippocampus of aged human brains, further suggesting its pathological role in neurodegeneration. Despite these findings, the molecular mechanisms by which activated TRPV4 regulates downstream target molecules and signaling pathways to induce microglial M1 polarization remain insufficiently understood. Animal studies have demonstrated that TRPV4 overactivation is a common pathological feature in AD models, where it disrupts calcium homeostasis in key brain regions, impairs synaptic plasticity, exacerbates oxidative stress, promotes Aβ plaque deposition, and compromises neuronal cytoskeleton integrity [15,17]. Nevertheless, limited studies have directly examined whether TRPV4-mediated microglial M1 polarization contributes to AD onset and progression or whether it leads to extensive neuronal apoptosis.

Consequently, this study aimed to investigate the potential mechanisms by which TRPV4 regulates M1-type microglia activation using an *in vitro* cell model and to further explore its specific effects on neurons. On one hand, this study elucidated how aberrant TRPV4 activation influences microglia and neuronal function, providing a novel perspective on the pathogenesis of AD. On the other hand, it identified specific downstream target molecules regulated by TRPV4, offering a theoretical foundation for the development of AD therapeutic strategies targeting these molecules.

Materials and Methods

Cell Culture

The BV-2 microglial and HT22 neuronal cell lines, both of murine origin, were obtained from the American Type Culture Collection (ATCC, Manassas, VA, USA) and used as *in vitro* cell models. Before experimentation, both cell lines underwent short tandem repeat (STR) profiling and mycoplasma testing to confirm authenticity and sterility. Only cells testing negative were used in all procedures. BV-2 and HT22 cells were cultured in high-glucose Dulbecco's Modified Eagle Medium (DMEM, Batch No. 20240315, Capricorn Scientific, Ebsdorfergrund, Germany) supplemented with 10% fetal bovine serum (FBS, Batch No. 20240320, Servicebio, Wuhan, China), 1% penicillin-streptomycin solution (Batch No. 20240325, Servicebio, Wuhan, China), and 1% glutamine (Batch No. 20240328, Servicebio, Wuhan, China). Cultures were maintained at 37 °C in a humidified atmosphere with 5% CO_2. The DMEM medium was replaced every 2 to 3 days, and cell morphology and density were monitored using an inverted optical microscope (IX73, Olympus, Tokyo, Japan). Once cells reached 70%–80% confluence, they were passaged or reseeded to maintain optimal growth conditions.

Experimental Reagents, Treatment Protocols, and Grouping

Solid lipopolysaccharide (LPS; Batch No. 20240318, Sigma-Aldrich, St. Louis, MO, USA), TRPV4 agonist GSK1016790A (Batch No. 20240320), and TRPV4 antagonist HC-067047 (Batch No. 20240322) were purchased from MedChemExpress (Monmouth Junction, NJ, USA). Stock solutions were prepared by dissolving each compound in 0.5% dimethyl sulfoxide (DMSO) according to the manufacturer's recommendations. These stocks were diluted with sterile phosphate-buffered saline (PBS) to final working concentrations of 10 µg/mL for LPS, 25 µM for GSK1016790A, and 2 µM for HC-067047. Dai *et al.* [18] demonstrated that a 10 µg/mL LPS effectively activates BV-2 cells; Fukuda *et al.* [19] reported that 25 µM GSK1016790A significantly activates TRPV4 channel, enhancing microglial pro-inflammatory responses; and Redmon *et al.* [20] showed that 2 µM HC-067047 sufficiently inhibits TRPV4 channel, preventing hypotonicity-induced microglial swelling. These concentrations were therefore adopted for this experiment.

Additionally, recombinant human transforming growth factor-beta 1 (TGF-β1; Batch No. 20240325, PeproTech, Rocky Hill, NJ, USA) in solid form was obtained from Biolab Biotechnology Co., Ltd. (Beijing, China). It was dissolved in double-distilled water to prepare a working solution of 10 ng/mL, following the protocol of da Silva *et al.* [21], who used this concentration for *in vitro* interventions in retinal Muller glial cells.

BV-2 cells were subjected to treatments with LPS, GSK1016790A, HC-067047, and TGF-β1 under various conditions and categorized into the following experimental groups: (1) Control group: BV-2 cells cultured under standard conditions for 24 hours; (2) LPS group: BV-2 cells treated with 10 µg/mL LPS for 24 hours; (3) LPS + GSK group: BV-2 cells pretreated with 25 µM GSK1016790A for 6 hours, then exposed to LPS for 24 hours; (4) LPS + HC group: BV-2 cells pretreated with 2 µM HC-067047 for 6 hours, followed by LPS treatment for 24 hours; (5) LPS + TGF-β1 group: BV-2 cells pretreated with 10 ng/mL TGF-β1 for 6 hours, followed by LPS treatment for 24 hours; and (6) LPS + GSK + TGF-β1 group: BV-2 cells pretreated with HC-067047 and TGF-β1 for 6 hours, followed by LPS treatment for 24 hours.

Following treatment, BV-2 cell supernatants were collected and used as conditioned media for culturing HT22 cells based on the methods described by Liu *et al.* [22]. Briefly, the supernatant was aspirated, centrifuged at 1000 ×g for 10 minutes at 4 °C, and passed through a 0.22 µm filter to eliminate residual cellular debris. HT22 cells were seeded in high-glucose DMEM at a density of 4×10^5 cells/mL and cultured until 90% confluence. At this point, the medium was replaced with 100 µL of the filtered conditioned medium, and the cells were incubated for an additional 48 hours at 37 °C in a humidified atmosphere containing 5% CO_2.

Detection of Phagocytic Activity

The phagocytic capacity of BV-2 cells was evaluated following the protocol of Lindner *et al.* [23]. Briefly, 2 µL of pHrodo™ Red Zymosan BioParticles™ Conjugates (#P35364, ThermoFisher Scientific, Waltham, MA, USA) were added to each well containing treated BV-2 cells and incubated at 37 °C for 1 hour. After incubation, cells were washed three times with PBS to remove unbound particles. Fluorescence intensity was then detected using an Infinite F50 microplate reader (TECAN, Serial No. 20240328, Männedorf, Switzerland) at 560 nm excitation and 585 nm emission wavelengths. Each condition was evaluated in three independent biological replicates (n = 3), with each replicate derived from separately cultured and treated BV-2 cells. The average value from the biological replicates was considered the final result.

Enzyme-linked Immunosorbent Assay

The supernatants from each group of treated BV-2 cells were collected following centrifugation at 12,000 ×g for 10 minutes at 4 °C. Levels of inducible nitric oxide synthase (iNOS, #SP14401), tumor necrosis factor-alpha (TNF-α, #SP13726), interleukin-1 beta (IL-1β, #SP12667), and interleukin-6 (IL-6, #SP13755) were quantified using commercial enzyme-linked immunosorbent assay (ELISA) kits (Batch No. 20240405, Saipei Biotechnology Co., Ltd., Wuhan, China). Each experimental group was tested using three independent biological replicates, with each replicate representing a separately cultured and treated population of BV-2 cells. The mean of the three replicates was considered the final result.

Immunofluorescence Assay

BV-2 cells from each treatment group were washed twice with PBS and then fixed in 4% paraformaldehyde at room temperature for 30 minutes. Cells were permeabilized with 0.1% Triton X-100 for 10 minutes, followed by blocking with 3% bovine serum albumin at ambient temperature for 30 minutes to minimize nonspecific binding. Primary antibodies were then applied for overnight incubation at 4 °C, including ionized calcium-binding adaptor molecule 1 (Iba-1, 1:300, #ab178846), CD86 (1:200, #ab119857), and CD206 (1:200, #ab64693), all from Abcam (Cambridge, UK). The following day, cells were washed with PBS and incubated for 1 hour in the dark with species-specific secondary antibodies, including goat anti-rabbit IgG Alexa Fluor® 488 (Cat# A-11008) and goat anti-rat Immunoglobulin G (IgG) Alexa Fluor® 594 (Cat# A-11007), both from Thermo Fisher Scientific (Waltham, MA, USA). Fluorescent imaging was performed using a fluorescence microscope (Nikon Eclipse C1, Nikon, Tokyo, Japan) to iden-

tify and capture Iba-1^{+}CD86^{+} and Iba-1^{+}CD206^{+} cells. Semi-quantitative analysis of M1 and M2 phenotypic proportions was performed using ImageJ software (version 1.54, NIH, Bethesda, MD, USA). All analyses were based on three independent biological replicates, each derived from individually cultured and treated BV-2 samples. The mean of these replicates was considered the final result.

Western Blot Assay

Cytoplasmic and nuclear proteins were extracted from BV-2 cells in each treatment group using a Nuclear and Cytoplasmic Protein Extraction Kit (#HZW4512, Shanghai Huzheng, Shanghai, China), following the manufacturer's protocol. Total protein concentrations were quantified using a bicinchoninic acid (BCA) assay kit (Beyotime Biotechnology, Shanghai, China). Equal amounts of protein were separated by 10% sodium dodecyl sulfate–polyacrylamide gel electrophoresis (SDS-PAGE) and transferred onto polyvinylidene fluoride (PVDF) membranes (Servicebio, Wuhan, China). Membranes were blocked with 5% skim milk at room temperature for 1 hour, then incubated overnight at 4 °C with the corresponding primary antibodies. The primary antibodies used included: iNOS (1:1000, #ab178945, Abcam, Cambridge, UK), cyclooxygenase-2 (COX-2, 1:1000, #ab179800, Abcam, Cambridge, UK), arginase-1 (Arg-1, 1:1000, #ab315110, Abcam, Cambridge, UK), interleukin-10 (IL-10, 1:1000, #ab310329, Abcam, Cambridge, UK), TGF-β1 (1:1000, #ab215715, Abcam, Cambridge, UK), IκBα (1:1000, #9242, Cell Signaling Technology, Danvers, MA, USA), p-IκBα (1:1000, #2859, Cell Signaling Technology, Danvers, MA, USA), p65 (1:1000, #8242, Cell Signaling Technology, Danvers, MA, USA), p-p65 (1:1000, #3033, Cell Signaling Technology, Danvers, MA, USA), β-actin (1:5000, #ab8227, Abcam, Cambridge, UK), and Histone H3 (1:5000, #ab1791, Abcam, Cambridge, UK). On the following day, membranes were washed three times with Tris-buffered saline containing Tween-20 and incubated for 1 hour at room temperature with horseradish peroxidase (HRP)-conjugated goat anti-rabbit IgG (Cat# GB23303, Servicebio, Wuhan, China). Detection of protein bands was performed using the Odyssey Infrared Imaging System (Li-Cor, Lincoln, NE, USA). Semi-quantitative band analysis was conducted using ImageJ software (version 1.54, NIH, Bethesda, MD, USA). Expression of cytoplasmic proteins was normalized to β-actin, while nuclear proteins were normalized to Histone H3. Each experimental group was evaluated using three independent biological replicates (n = 3), with each replicate representing a distinct BV-2 culture and treatment. The mean value of these replicates was used as the final result.

TRPV4 protein expression was not measured, as its activity was directly modulated using pharmacological agonists and antagonists. Previous studies have shown that TRPV4 activity can be effectively regulated through such means without altering its expression levels [24].

Cell Viability Assay

HT22 cell viability was measured using the MTT assay. Following treatment, 10 µL of a 5 mg/mL MTT working solution was added to each well and incubated for 4 hours to allow for formazan crystal formation. After incubation, supernatants were discarded, and 150 µL of dimethyl sulfoxide (DMSO) was added to each well to solubilize the dye, followed by gentle shaking to ensure complete dissolution of the crystals. Absorbance was subsequently measured at 570 nm using the Infinite F50 microplate reader (TECAN, Serial No. 20240328, Männedorf, Switzerland) to evaluate cell viability. Each condition was assessed in three independent biological replicates, with each replicate involving separately treated HT22 cultures exposed to conditioned medium. The mean value from the replicates was considered the final result.

Terminal Deoxynucleotidyl Transferase dUTP Nick End Labeling (TUNEL) Staining

Apoptotic levels in HT22 cells were assessed using the TUNEL assay. After culture, cells were rinsed twice with PBS, fixed in 4% paraformaldehyde at room temperature for 30 minutes, and permeabilized with 0.1% Triton X-100 for 10 minutes. The permeabilized cells were then incubated in the dark at room temperature for 1 hour with a fluorescein isothiocyanate (FITC)-labeled TUNEL Cell Apoptosis Detection Kit (#G1501-100T, Servicebio, Wuhan, China). Nuclear counterstaining was performed using 4′,6-diamidino-2-phenylindole (DAPI) for 10 minutes to visualize nuclei. Fluorescence microscopy was utilized to capture images, and the percentage of TUNEL-positive cells was quantified using ImageJ software (NIH, Bethesda, MD, USA) to evaluate apoptotic levels. Analysis was based on three independent biological replicates (n = 3), with each replicate involving a separately treated HT22 cell culture exposed to conditioned media. The mean value of these biological replicates was used as the final result.

Statistical Analysis

Data are presented as mean ± standard deviation (SD). Statistical analyses were performed using SPSS version 24.0 (IBM Corp., Armonk, NY, USA). The Shapiro–Wilk test was initially applied to assess data normality, and the results indicated an approximately normal distribution. A one-way analysis of variance (ANOVA) was used to detect differences among groups, followed by Tukey's post hoc test for pairwise comparisons. All analyses were performed using three biological replicates (n = 3), not merely technical replicates. Each biological replicate was derived from independently cultured and treated cell samples. Values were reported as mean ± SD, and a p-value < 0.05 was considered statistically significant.

Results

TRPV4 Facilitates the Upregulation of Phagocytic Activity and Inflammatory Cytokine Expression in Lipopolysaccharide-stimulated BV-2 Cells

Initially, we investigated the effects of TRPV4 on the phagocytic capacity and inflammatory cytokine expression levels in microglial cells. The phagocytosis assay using pHrodo™ Red Zymosan BioParticles™ Conjugates demonstrated that LPS treatment significantly enhanced the phagocytic activity of BV-2 cells, an effect further amplified by the TRPV4 agonist GSK1016790A. In contrast, treatment with the TRPV4 inhibitor HC-067047 partially attenuated the LPS-induced influence on phagocytic be-

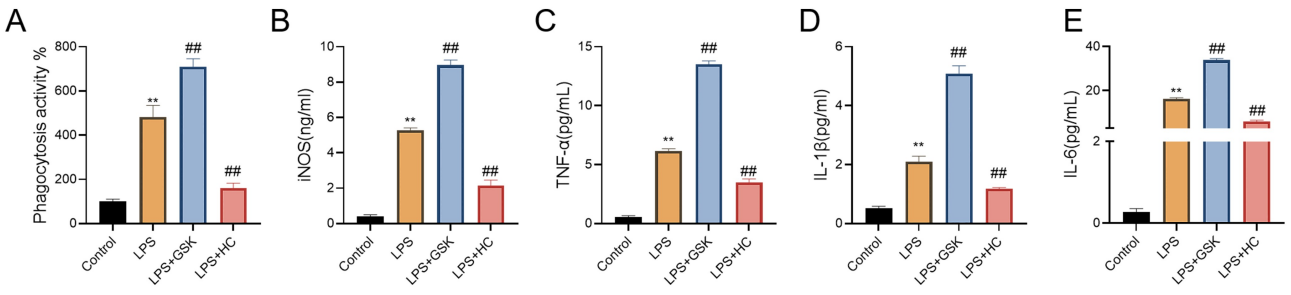

Fig. 1. TRPV4 activation enhances phagocytic activity and inflammatory cytokine release in BV-2 cells following lipopolysaccharide stimulation. (A) Phagocytic activity assessed using pHrodo™ Red Zymosan BioParticles™ Conjugates. (B–E) Quantification of inflammatory mediators iNOS, TNF-α, IL-1β, and IL-6 in the culture supernatant by ELISA. Abbreviations: TRPV4, transient receptor potential vanilloid 4; iNOS, inducible nitric oxide synthase; TNF-α, tumor necrosis factor alpha; IL-1β, interleukin-1 beta; IL-6, interleukin-6; ELISA, enzyme-linked immunosorbent assay; LPS, lipopolysaccharide. Data are presented as mean ± standard deviation (SD), n = 3. $^{**}p < 0.01$ vs. Control group; $^{\#\#}p < 0.01$ vs. LPS group.

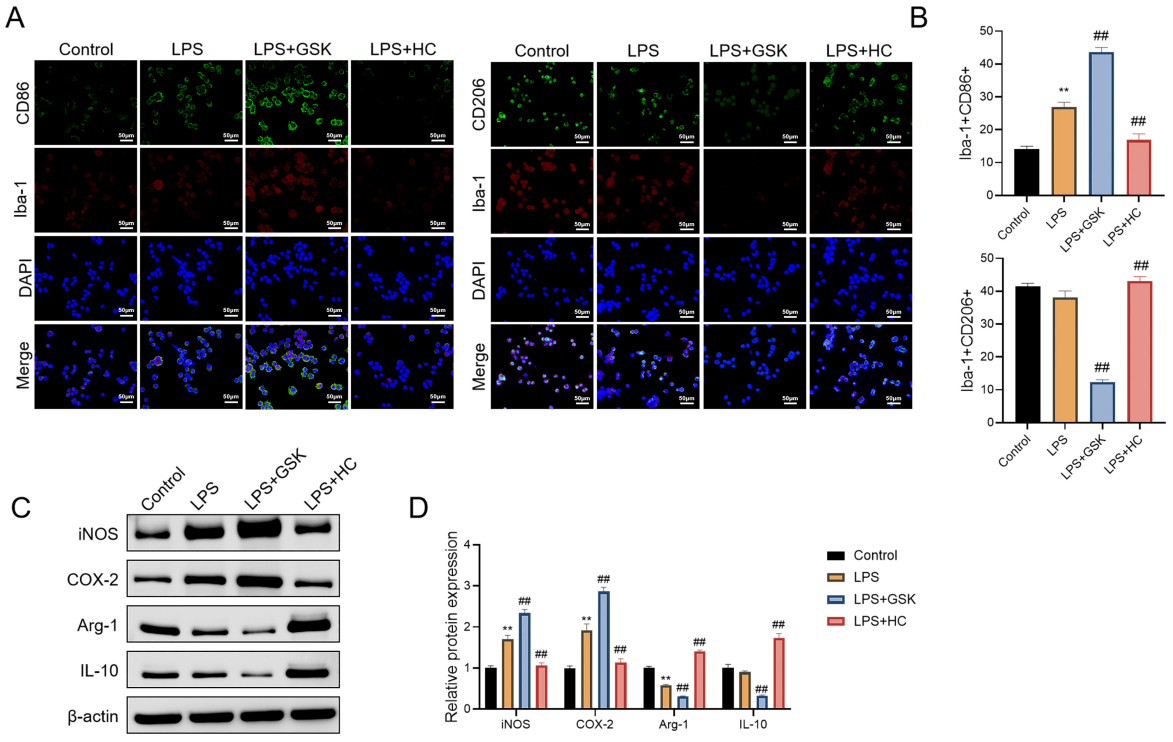

Fig. 2. TRPV4 activation promotes M1 polarization of BV-2 cells induced by lipopolysaccharide. (A) Immunofluorescence analysis of Iba-1, CD86, and CD206 expression. (B) Quantification of Iba-1^{+}CD86^{+} (M1) and Iba-1^{+}CD206^{+} (M2) cell. (C) Western blot analysis of M1 markers (iNOS, COX-2) and M2 markers (Arg-1 and IL-10). (D) Densitometric quantification of iNOS, COX-2, Arg-1, and IL-10 protein levels. Abbreviations: Iba-1, ionized calcium-binding adaptor molecule 1; iNOS, inducible nitric oxide synthase; COX-2, cyclooxygenase-2; Arg-1, arginase-1; IL-10, interleukin-10; DAPI, 4′,6-diamidino-2-phenylindole. Data are presented as mean ± SD, n = 3. $^{**}p < 0.01$ vs. Control group; $^{\#\#}p < 0.01$ vs. LPS group.

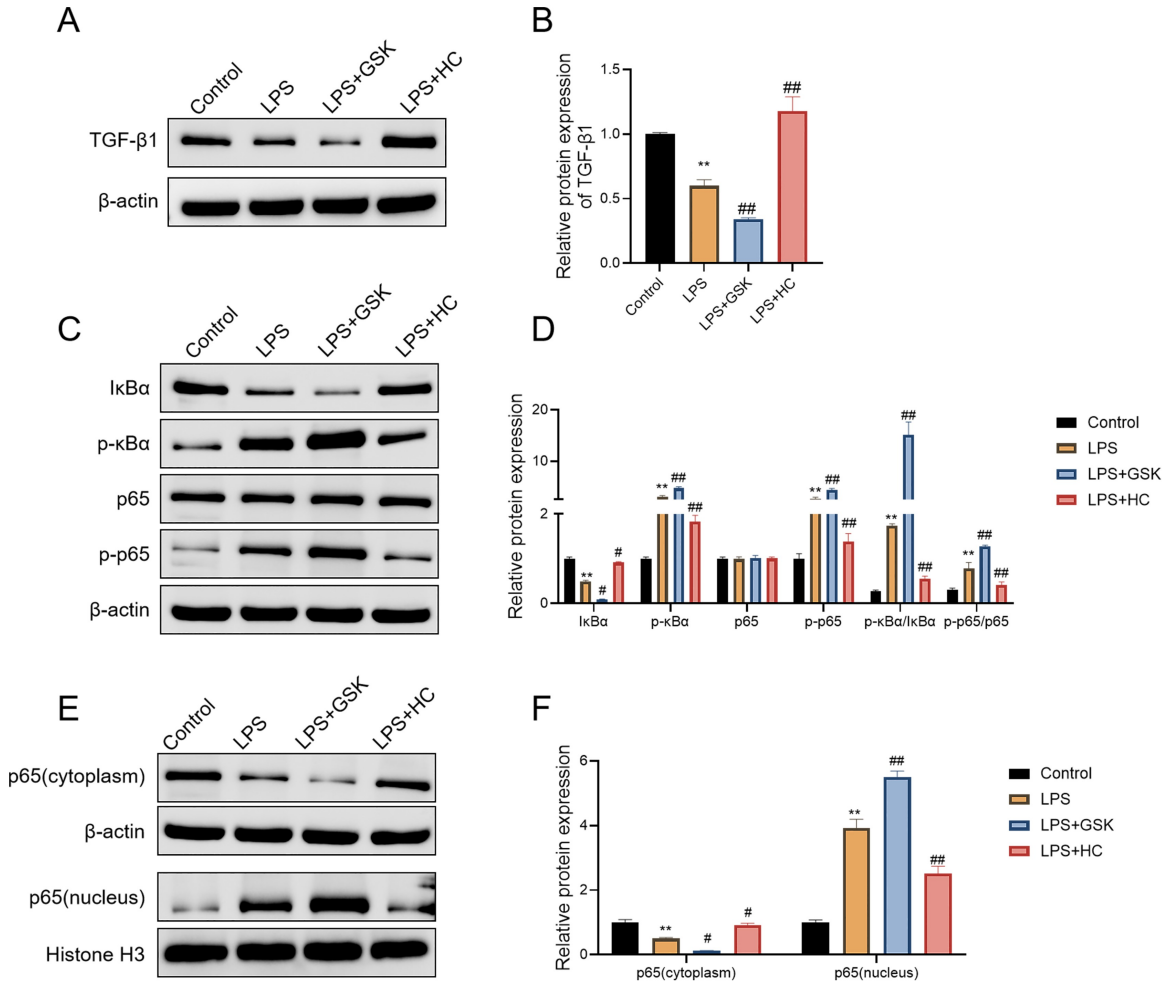

Fig. 3. TRPV4 downregulates TGF-β1 to activate the NF-κB pathway in lipopolysaccharide-stimulated BV-2 cells. (A) Western blot analysis of TGF-β1 protein levels in BV-2 cells. (B) Quantification of TGF-β1 protein levels. (C) Western blot analysis of IκBα, p-IκBα, p65, and p-p65 protein levels in BV-2 cells. (D) Quantitative analysis of total and phosphorylated IκBα and p65, including p-IκBα/IκBα and p-p65/p65 ratios. (E) Western blot analysis of nuclear and cytoplasmic p65 levels in BV-2 cells. (F) Quantification of nuclear and cytoplasmic p65 protein levels. Abbreviations: TGF-β1, transforming growth factor-beta 1. Data are presented as mean $\pm$ SD, n = 3. $^{**}p < 0.01$ vs. Control group; $^{\#}p < 0.05$, $^{\#\#}p < 0.01$ vs. LPS group.

havior of BV-2 cells (Fig. 1A,B) ($p < 0.01$). Enzyme-linked immunosorbent assay (ELISA) demonstrated that LPS stimulation significantly enhanced the secretion of iNOS, TNF-α, IL-1β, and IL-6 into the culture supernatant. These cytokine levels were further elevated upon TRPV4 activation by GSK1016790A, while HC-067047 markedly suppressed the LPS-induced inflammatory response (Fig. 1C–E) ($p < 0.01$). These findings suggest that TRPV4 activation enhances both the phagocytic activity and pro-inflammatory cytokine secretion by BV-2 cells following LPS stimulation.

TRPV4 Promotes the Polarization of Lipopolysaccharide-induced BV-2 Cells Toward the M1 Phenotype

To further investigate whether TRPV4 regulates the polarization phenotype of microglial cells, we analyzed the expression of M1 and M2 phenotype markers in BV-2 cells using immunofluorescence and Western blot assays. Immunofluorescence results revealed that LPS treatment significantly increased the number of Iba-1^{+}CD86^{+} (M1) cells while slightly reducing the Iba-1^{+}CD206^{+} (M2) population. These effects were further amplified by GSK1016790A but were partially reversed by HC-067047 (Fig. 2A,B) ($p < 0.01$).

Western blot analysis revealed that LPS treatment significantly increased M1 phenotype markers (iNOS and COX-2) and reduced M2 markers (Arg-1 and IL-10).

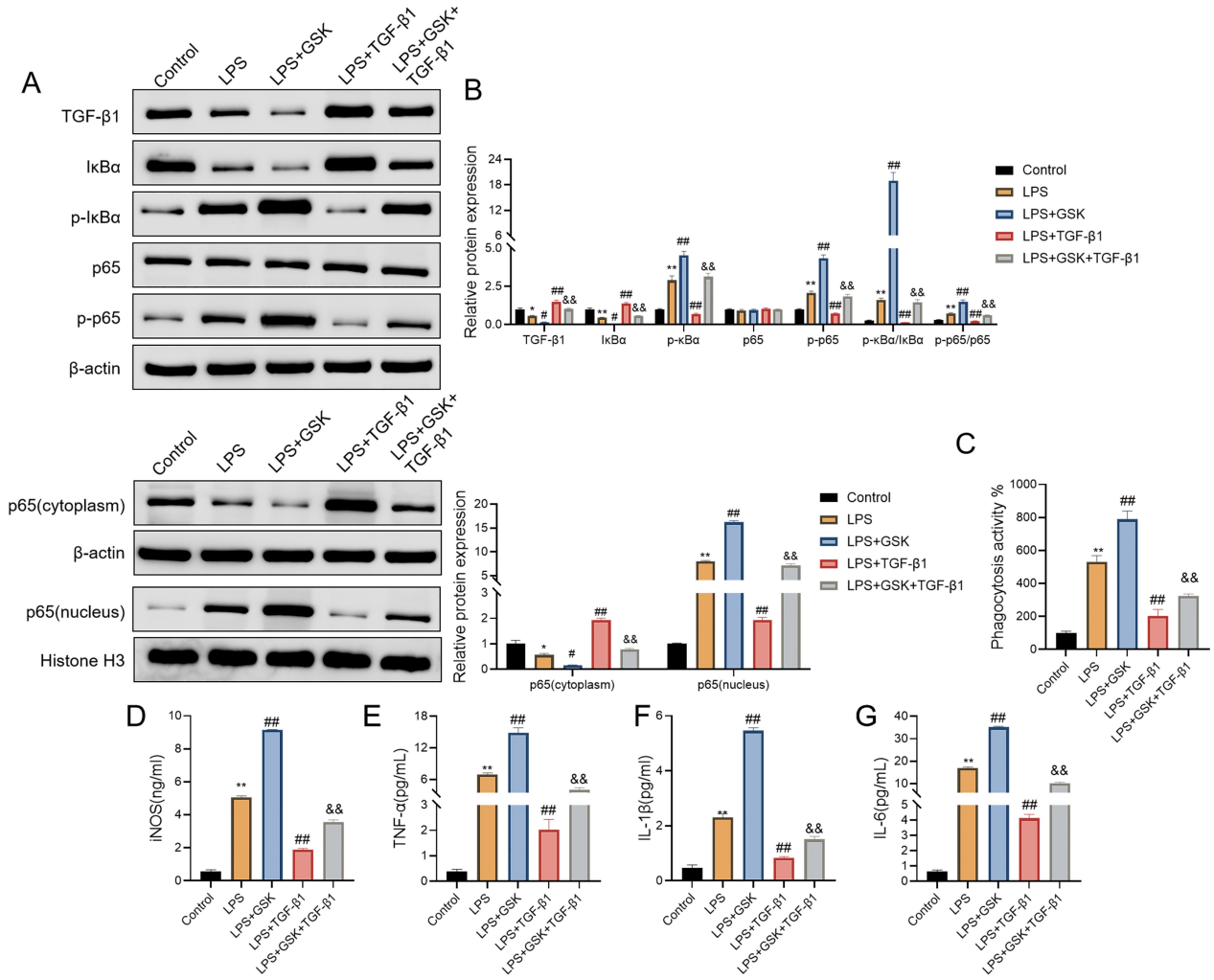

Fig. 4. TGF-β1 reverses the effects of TRPV4 activation on lipopolysaccharide-induced phagocytic activity and inflammatory cytokine release in BV-2 cells. (A) Western blot analysis of TGF-β1, IκBα, p-IκBα, p65, p-p65, and subcellular p65 protein levels (nuclear and cytoplasmic). (B) Quantitative analysis of TGF-β1, IκBα, p-IκBα, p65, and p-p65 protein levels, along with phosphorylation ratios (p-IκBα/IκBα and p-p65/p65). (C) Phagocytic activity was assessed via fluorescent microsphere uptake. (D–G) ELISA quantification of iNOS, TNF-α, IL-1β, and IL-6 in the culture supernatant. Abbreviations: TGF-β1, transforming growth factor-beta 1; ELISA, enzyme-linked immunosorbent assay; iNOS, inducible nitric oxide synthase; TNF-α, tumor necrosis factor alpha; IL-1β, interleukin-1 beta; IL-6, interleukin-6. Data are presented as mean $\pm$ SD, n = 3. $^{*}p < 0.05$, $^{**}p < 0.01$ vs. Control group; $^{\#}p < 0.05$, $^{\#\#}p < 0.01$ vs. LPS group; $^{\&\&}p < 0.01$ vs. LPS + TGF-β1 group.

These changes were further enhanced by TRPV4 activation through GSK1016790A and were notably reversed by HC-067047 (Fig. 2C,D) ($p < 0.01$). Together, these results indicate that TRPV4 activation significantly promotes the M1 polarization of BV-2 cells under LPS stimulation.

TRPV4 Downregulates TGF-β1 Protein to Activate the NF-κB Pathway in Lipopolysaccharide-stimulated BV-2 Cells

Given the observed effect of TRPV4 on microglial polarization, we investigated the underlying mechanisms. Western blot analysis demonstrated that LPS stimulation significantly reduced TGF-β1 protein expression, suppressed IκBα levels, and increased phosphorylation of IκBα (p-IκBα) and p65 (p-p65), along with enhanced nuclear translocation of p65. These effects were further amplified by GSK1016790A, whereas HC-067047 significantly alleviated these alterations (Fig. 3A–F) ($p < 0.05$). These findings suggest that TRPV4 activation promotes LPS-induced NF-κB signaling by downregulating TGF-β1 expression in BV-2 cells.

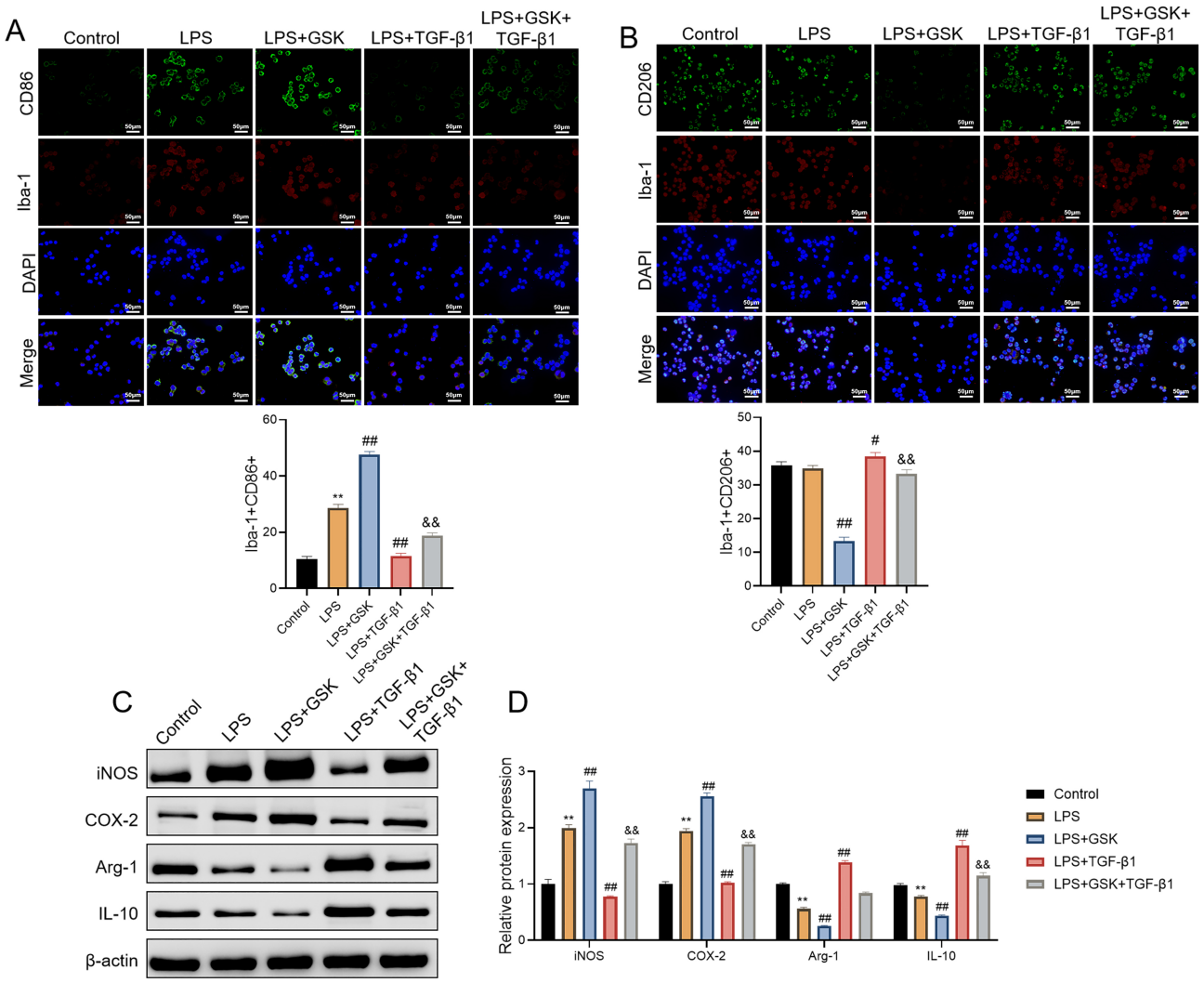

Fig. 5. TGF-β1 reverses the effects of TRPV4 activation on lipopolysaccharide-induced M1 polarization of BV-2 cells. (A) Immunofluorescence staining of Iba-1, CD86, and CD206 to evaluate microglial polarization. (B) Quantification of Iba-1$^+$CD86$^+$ (M1) and Iba-1$^+$CD206$^+$ (M2) microglial populations. (C) Western blot analysis of iNOS, COX-2 (M1 markers), Arg-1, and IL-10 (M2 markers). (D) Densitometric quantification of iNOS, COX-2, Arg-1, and IL-10 protein levels. Abbreviations: Iba-1, ionized calcium-binding adaptor molecule 1; iNOS, inducible nitric oxide synthase; COX-2, cyclooxygenase-2; Arg-1, arginase-1; IL-10, interleukin-10. Data are expressed as mean $\pm$ SD, n = 3. $^{**}p < 0.01$ vs. Control group; $^{\#}p < 0.05$, $^{\#\#}p < 0.01$ vs. LPS group; $^{\&\&}p < 0.01$ vs. LPS+TGF-β1 group.

TGF-β1 Reverses the Effects of TRPV4 on Lipopolysaccharide-induced Phagocytic Activity, Inflammatory Cytokine Release, and M1 Phenotype Marker Levels in BV-2 Cells

Since TRPV4 activation downregulated TGF-β1 protein levels, we further investigated whether exogenous TGF-β1 could reverse the effects of TRPV4 on BV-2 cells. Western blot analysis showed that exogenous TGF-β1 significantly reversed the modulatory effects of LPS and GSK1016790A on the NF-κB signaling pathway. Specifically, exogenous TGF-β1 upregulated IκBα protein expression, reduced p-IκBα and p-p65 levels, and inhibited p65 nuclear translocation (Fig. 4A,B) ($p < 0.05$). Additionally, phagocytosis assays using fluorescent microspheres, along with ELISA, demonstrated that exogenous TGF-β1 markedly counteracted the effects of LPS and GSK1016790A on the phagocytic activity and inflammatory cytokine secretion in BV-2 cells. These effects were characterized by a substantial impairment in the microsphere-engulfing ability of BV-2 cells and a marked decrease in the secretion of inflammatory mediators, including iNOS, TNF-α, IL-1β, and IL-6 in the supernatant (Fig. 4C–G) ($p < 0.01$).

Subsequent immunofluorescence and Western blot analyses revealed that exogenous TGF-β1 significantly reversed the effects of LPS and GSK1016790A on M1 and M2 phenotype marker expression in BV-2 cells. These changes were evidenced by a marked decrease in Iba-

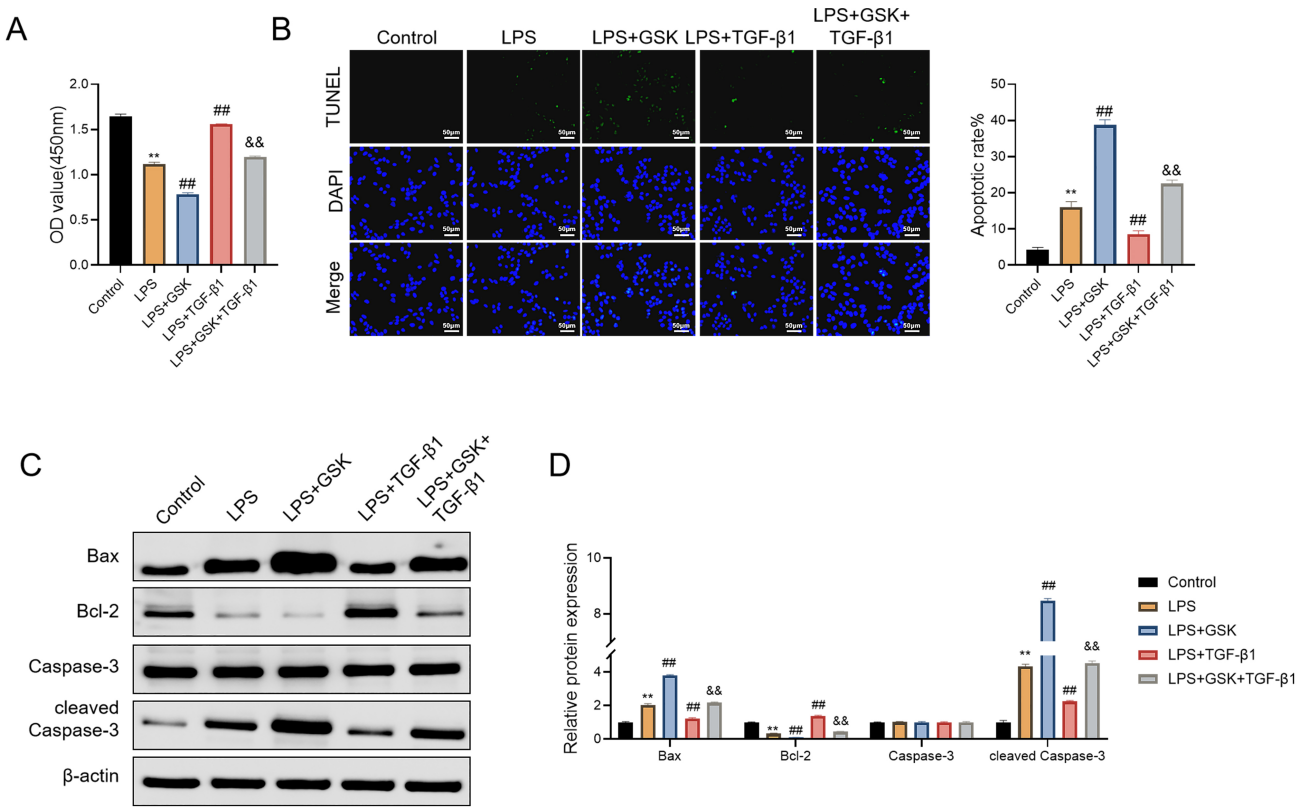

Fig. 6. TRPV4 suppresses HT22 cell viability and promotes apoptosis by downregulating TGF-β1. (A) MTT assay evaluating the viability of HT22 hippocampal neurons. (B) TUNEL assay assessing apoptotic cell death in HT22 cells. (C) Western blot analysis of apoptotic markers, including Bax, Bcl-2, Caspase-3, and cleaved Caspase-3 protein levels in HT22 cells. (D) Quantification of Bax, Bcl-2, Caspase-3, and cleaved Caspase-3 protein levels. Abbreviations: TUNEL, terminal deoxynucleotidyl transferase dUTP nick end labeling; DAPI, 4′,6-diamidino-2-phenylindole; OD, Optical Density; Bcl-2, B-cell lymphoma-2. Data are presented as mean $\pm$ SD, n = 3. $^{**}p < 0.01$ vs. Control group; $^{\#\#}p < 0.01$ vs. LPS group; $^{\&\&}p < 0.01$ vs. LPS + TGF-β1 group.

$1^{+}CD86^{+}$ cells, a significant increase in Iba-$1^{+}CD206^{+}$ cells, a decrease in iNOS and COX-2 protein levels, and an increase in Arg-1 and IL-10 protein expression levels (Fig. 5A–D) ($p < 0.05$).

Collectively, these observations suggest that TGF-β1 inhibits the NF-κB signaling pathway, reversing the TRPV4-induced increase in LPS-stimulated phagocytic activity and inflammatory cytokine release in BV-2 cells while reducing intracellular M1 phenotype marker expression. Overall, exogenous TGF-β1 significantly reverses TRPV4-induced M1 polarization of BV-2 cells.

TRPV4 Suppresses HT22 Cell Viability and Promotes Apoptosis by Downregulating TGF-β1

Finally, we evaluated the effects of TRPV4 activation and exogenous TGF-β1 on HT22 cells. MTT assay results demonstrated that LPS treatment significantly reduced HT22 cell viability, and this reduction was further exacerbated by GSK1016790A. In contrast, exogenous TGF-β1 reversed these effects, significantly restoring cell viability (Fig. 6A) ($p < 0.01$).

Similarly, TUNEL staining revealed that LPS treatment elevated the apoptosis level in HT22 cells, an effect further enhanced by GSK1016790A. However, exogenous TGF-β1 reversed this pro-apoptotic effect, significantly reducing the number of TUNEL-positive cells (Fig. 6B) ($p < 0.01$).

Consistent with these results, Western blot analysis of apoptosis-related proteins revealed elevated expression of pro-apoptotic Bax and cleaved Caspase-3, along with reduced levels of anti-apoptotic B-cell lymphoma-2 (Bcl-2) in LPS-treated HT22 cells. These effects were further enhanced by GSK1016790A whereas exogenous TGF-β1 reversed the effects by reducing Bax and cleaved Caspase-3 levels and increasing Bcl-2 expression in HT22 cells (Fig. 6C,D) ($p < 0.01$).

Collectively, these findings indicate that TRPV4 activation suppresses HT22 cell viability and promotes apoptosis, effects that are significantly reversed by exogenous TGF-β1. In summary, TRPV4 exerts its pro-apoptotic effects in HT22 cells by downregulating TGF-β1 expression.

Discussion

Our *in vitro* experiments demonstrated that TRPV4 activation significantly enhanced microglial polarization toward the pro-inflammatory M1 phenotype. This effect was likely mediated by the downregulation of TGF-β1 expression and activation of the NF-κB signaling pathway, ultimately aggravating neuronal apoptosis. Based on the available literature, this study provides the first evidence linking TRPV4 activation to the regulation of TGF-β1 protein levels and the NF-κB signaling pathway activation in microglia. These findings offer new insights into the mechanisms underlying microglia-mediated neuroinflammation and neuronal damage during the pathological progression of AD. Clinically, our study further demonstrated that exogenous administration of TGF-β1 effectively reversed the adverse effects of TRPV4 activation. This suggests that TGF-β1-based interventions may help mitigate excessive neuronal apoptosis in AD patients, offering a promising direction for the development of novel therapeutic strategies for AD.

A prominent pathological feature of AD is a sustained neuroinflammatory response [25]. However, replicating the complex chronic neuroinflammatory environment observed in the AD brain using *in vitro* models remains a significant challenge. To address this, we used the classical inflammatory inducer lipopolysaccharide (LPS) to stimulate BV-2 cells, aiming to simulate the chronic inflammatory stimuli experienced by microglia in the AD brain. Following LPS exposure, we observed a significant increase in the phagocytic activity of BV-2 cells, elevated release of pro-inflammatory cytokines, reduced expression of M2 phenotype markers (CD206, Arg-1, and IL-10), and enhanced expression of M1 phenotype markers (CD86, iNOS, and COX-2) [26,27]. These results indicated that LPS induced a phenotypic shift in BV-2 cells from M2 to M1 phenotype. Previous studies have similarly reported that LPS exposure leads to microglial swelling, sustained M1 polarization, and the release of neurotoxic molecules [28–30], which is consistent with our findings.

Another key challenge of this study was how to effectively modulate TRPV4 activity *in vitro* to comprehensively investigate its functional roles from both activating and inhibitory perspectives. Song *et al*. [31] observed that TRPV4 expression was significantly upregulated in liver tissues of A CCl_4-induced rat model of liver fibrosis, while Lee and Choe [17] reported elevated TRPV4 expression in the cortex, hippocampus, cerebellum, and spinal cord of aged rats. Nevertheless, these expression changes occur primarily under specific pathological conditions and are likely regulated by complex factors *in vivo*. Moreover, existing evidence suggests that TRPV4, as a channel protein, generally exhibits relatively stable expression, making it challenging to achieve substantial modulation through direct genetic manipulation or pharmacological intervention [32]. Notably, the function of TRPV4 is largely determined by its activation state rather than its absolute expression levels [24]. Therefore, in this study, rather than directly modulating TRPV4 expression, we opted to use the agonist GSK1016790A and the antagonist HC-067047 to activate and inhibit TRPV4, respectively, in order to examine its effects on microglia and neurons. During the experimental group design, we briefly considered including a GSK1016790A-only group (i.e., TRPV4 activation without LPS stimulation). However, preliminary tests revealed that TRPV4 activation alone did not induce significant changes in microglial polarization or cytokine secretion under basal conditions. These observations suggest that TRPV4 may require a pro-inflammatory background to exert its modulatory effects. Therefore, we included LPS stimulation in all TRPV4-related groups to better simulate the chronic neuroinflammatory environment characteristic of neurodegenerative diseases such as AD.

In this study, we demonstrated the role of TRPV4 activation in promoting microglial M1 polarization from three complementary perspectives. First, the co-culture of BV-2 cells with fluorescently labeled conjugates revealed that TRPV4 activation via GSK1016790A significantly enhanced the phagocytic activity of BV-2 cells. Previous studies have shown that abnormally enhanced phagocytic activity is a hallmark of M1-type microglia. In the AD brain, M1-polarized microglia uncontrollably engulf healthy synapses, impairing neurotransmitter transport and neuronal signaling, which ultimately aggravates learning and memory disorders in AD patients [33]. Second, we observed that activation of TRPV4 by GSK1016790A significantly increased the secretion of multiple pro-inflammatory cytokines into the culture supernatant. Notably, the persistent release of inflammatory mediators is a critical mechanism by which M1-type microglia maintain chronic neuroinflammation and contribute to AD pathology [11]. Third, GSK1016790A stimulation led to a marked increase in CD86-positive microglia and elevated intracellular iNOS and COX-2, which are recognized markers of the M1-type microglia [26,27]. In contrast, inhibition of TRPV4 using HC-067047 produced the opposite effects across all these parameters. Collectively, evidence from these three perspectives strongly supports that TRPV4 activation promotes the transition of microglia to the pro-inflammatory M1 phenotype, whereas TRPV4 inhibition facilitates their transition toward the anti-inflammatory M2 phenotype.

In addition, Fukuda *et al*. [19], using *in vitro* experiments, demonstrated that low-temperature exposure could inactivate TRPV4, thereby inhibiting the M1 polarization of microglia. Similarly, Ren *et al*. [34] reported that acupuncture suppressed TRPV4 activity in the brains of ischemic stroke rat models, reducing the proportion of M1-type microglia. Furthermore, Liu *et al*. [35] reported that dexmedetomidine alleviated the rate of microglial M1 polarization by blocking TRPV4-induced calcium influx, re-

sulting in potent analgesic effects. These findings are in agreement with the conclusions of the present study.

After confirming the regulatory role of TRPV4 in microglial M1 polarization, we further investigated the underlying mechanism, primarily focusing on the NF-κB signaling pathway. NF-κB is a highly conserved pathway that remains inactive in the cytoplasm under basal conditions, where it forms a complex with IκB. Upon stimulation, IκBα undergoes phosphorylation and rapid degradation, allowing NF-κB, with p65 as a key subunit, to translocate into the nucleus and drive the induction of downstream inflammatory genes [36]. Notably, the NF-κB signaling pathway has been shown to play a crucial role in exacerbating neuroinflammation in AD [37]. In this study, TRPV4 activation led to reduced IκBα protein levels, increased p-IκBα expression, and nuclear translocation of p65, collectively indicating activation of the NF-κB signaling pathway. These findings suggest that TRPV4 regulates microglial M1 polarization through modulation of the NF-κB signaling pathway. Subsequently, we investigated the downstream targets through which TRPV4 activates the NF-κB signaling pathway. Previous animal studies have suggested that TGF-β1 serves as an upstream regulator of the NF-κB pathway. Localized TGF-β1 administration in animal models has been shown to suppress the NF-κB signaling pathway, thereby preventing chondrocyte and neuronal pyroptosis as well as conferring therapeutic benefits in osteoarthritis and CNS demyelinating diseases [38,39]. Based on this evidence, we hypothesized that TGF-β1 may serve as the intermediary molecule linking TRPV4 to the NF-κB signaling pathway. Our experimental findings revealed that TRPV4 activation significantly reduced TGF-β1 protein expression, while exogenous TGF-β1 administration reversed TRPV4-induced NF-κB activation and neutralized its effects on microglia. These findings support our hypothesis that TRPV4 facilitates M1 polarization of BV-2 cells by downregulating TGF-β1 protein levels, which represents the primary novelty of this study.

As previously noted, microglial M1 polarization and the subsequent release of pro-inflammatory cytokines are critical mechanisms contributing to neuronal damage in various neurodegenerative disorders [11]. In this study, the conditioned medium derived from treated BV-2 cells was applied to HT22 cells to simulate the impact of activated microglia on hippocampal neurons in the brain. Our results demonstrated that activation of TRPV4 via GSK1016790A significantly reduced neuronal viability and induced apoptosis. However, the addition of TGF-β1 partially reversed the detrimental effects of TRPV4 activation on neurons. These findings suggest that TRPV4 contributes to hippocampal neuronal injury and AD progression by downregulating TGF-β1 expression.

The crucial discovery of this study is that TGF-β1 effectively mitigates microglial M1 polarization and neuronal damage induced by TRPV4 activation, providing theoretical support for the development of TGF-β1-based therapies for AD. Current clinical treatments for AD, such as acetylcholinesterase inhibitors and N-methyl-D-aspartate (NMDA) receptor antagonists, are primarily limited to symptomatic relief. Although these treatments may modestly slow cognitive decline, they do not directly target the pathological mechanisms of AD or reverse existing neuronal damage [40]. In contrast, our findings highlight the potential of TGF-β1-based strategies, which may provide enhanced efficacy by suppressing microglial M1 polarization and inhibiting NF-κB pathway activation, thereby mitigating inflammation and neuronal apoptosis at its origin. Additionally, compared to some costly and technology-intensive therapies, TGF-β1, as an endogenous protein, offers benefits such as established manufacturing protocols, lower production costs, and ease of administration. It is conceivable that localized injection or hippocampal-targeted delivery of TGF-β1 could emerge as a novel therapeutic approach for AD in the future.

Despite these significant findings, several limitations of this study must be acknowledged. First, all experiments were conducted *in vitro* using BV-2 microglial cells and HT22 hippocampal neuronal cells, which may not fully replicate the intricate nature of the *in vivo* brain microenvironment characteristic of Alzheimer's disease. Second, although we demonstrated the protective role of TGF-β1 against TRPV4-induced microglial activation and neuronal apoptosis, only a single concentration of TGF-β1 (10 ng/mL) was used. A comprehensive dose–response analysis is still lacking, which limits our understanding of the optimal therapeutic dose and potential saturation thresholds. Third, the present study focused primarily on the TRPV4/TGF-β1/NF-κB signaling axis. However, TRPV4 is known to interact with additional signaling pathways, such as MAPK and Ca^{2+}-dependent mechanisms, which were not explored in this work. Lastly, our conclusions are based predominantly on protein-level assessments and morphological observations. Additional functional assays and *in vivo* validations are needed to strengthen the translational relevance of our findings.

Conclusion

In summary, our study has identified a pivotal role for TRPV4 in regulating microglial polarization and neuronal survival. Using BV-2 cells as a microglial model and HT22 cells as a hippocampal neuronal model *in vitro*, we demonstrated that TRPV4 activation induces microglial polarization toward the pro-inflammatory M1 phenotype. This polarization was marked by enhanced phagocytic activity, elevated secretion of inflammatory cytokines, and upregulation of M1-specific markers. Moreover, the process involved activation of the NF-κB signaling pathway, leading to reduced neuronal viability and increased apoptosis in hippocampal neurons. Notably, exogenous TGF-β1 sup-

plementation was able to partially reverse these detrimental effects. These findings clarify the downstream molecular mechanisms underlying TRPV4-mediated microglial M1 polarization and provide a theoretical basis for developing AD therapies targeting TGF-β1. Future research should investigate the clinical potential of TGF-β1 as a component of therapeutic regimens for AD patients.

Availability of Data and Materials

The data used to support the findings of this study are available from the corresponding author upon request.

Author Contributions

TZ, Conceptualization, Formal analysis, Writing - original draft; RGZ, Formal analysis, Writing - original draft; CY, Data curation, Resources; JFW, Data curation, Investigation; YF, Methodology, Project administration, Funding acquisition, Supervision. All authors contributed to critical revision of the manuscript for important intellectual content. All authors given final approval of the version to be published; have agreed on the journal to which the article has been submitted; and agree to be accountable for all aspects of the work.

Ethics Approval and Consent to Participate

Not applicable.

Acknowledgment

Not applicable.

Funding

This study was supported by Scientific Research Projects from Wuhan Municipal Health Commission (No.WX21B25).

Conflict of Interest

The authors declare no conflict of interest.

References

[1] Abeysinghe AADT, Deshapriya RDUS, Udawatte C. Alzheimer's disease; a review of the pathophysiological basis and therapeutic interventions. Life Sciences. 2020; 256: 117996. https://doi.org/10.1016/j.lfs.2020.117996.

[2] Li R, Qi J, Yang Y, Wu Y, Yin P, Zhou M, *et al*. Disease Burden and Attributable Risk Factors of Alzheimer's Disease and Dementia in China from 1990 to 2019. The Journal of Prevention of Alzheimer's Disease. 2022; 9: 306–314. https://doi.org/10.14283/jpad.2021.69.

[3] 2023 Alzheimer's disease facts and figures. Alzheimer's & Dementia: the Journal of the Alzheimer's Association. 2023; 19: 1598–1695. https://doi.org/10.1002/alz.13016.

[4] Li X, Feng X, Sun X, Hou N, Han F, Liu Y. Global, regional, and national burden of Alzheimer's disease and other dementias, 1990-2019. Frontiers in Aging Neuroscience. 2022; 14: 937486. https://doi.org/10.3389/fnagi.2022.937486.

[5] Jeong S. Molecular and Cellular Basis of Neurodegeneration in Alzheimer's Disease. Molecules and Cells. 2017; 40: 613–620. https://doi.org/10.14348/molcells.2017.0096.

[6] Mangalmurti A, Lukens JR. How neurons die in Alzheimer's disease: Implications for neuroinflammation. Current Opinion in Neurobiology. 2022; 75: 102575. https://doi.org/10.1016/j.conb.2022.102575.

[7] Abubakar MB, Sanusi KO, Ugusman A, Mohamed W, Kamal H, Ibrahim NH, *et al*. Alzheimer's Disease: An Update and Insights Into Pathophysiology. Frontiers in Aging Neuroscience. 2022; 14: 742408. https://doi.org/10.3389/fnagi.2022.742408.

[8] Monteiro AR, Barbosa DJ, Remião F, Silva R. Alzheimer's disease: Insights and new prospects in disease pathophysiology, biomarkers and disease-modifying drugs. Biochemical Pharmacology. 2023; 211: 115522. https://doi.org/10.1016/j.bcp.2023.115522.

[9] Hansen DV, Hanson JE, Sheng M. Microglia in Alzheimer's disease. The Journal of Cell Biology. 2018; 217: 459–472. https://doi.org/10.1083/jcb.201709069.

[10] Edler MK, Mhatre-Winters I, Richardson JR. Microglia in Aging and Alzheimer's Disease: A Comparative Species Review. Cells. 2021; 10: 1138. https://doi.org/10.3390/cells10051138.

[11] Wang Q, Yao H, Liu W, Ya B, Cheng H, Xing Z, *et al*. Microglia Polarization in Alzheimer's Disease: Mechanisms and a Potential Therapeutic Target. Frontiers in Aging Neuroscience. 2021; 13: 772717. https://doi.org/10.3389/fnagi.2021.772717.

[12] Kulkarni B, Cruz-Martins N, Kumar D. Microglia in Alzheimer's Disease: An Unprecedented Opportunity as Prospective Drug Target. Molecular Neurobiology. 2022; 59: 2678–2693. https://doi.org/10.1007/s12035-021-02661-x.

[13] Liu N, Yan F, Ma Q, Zhao J. Modulation of TRPV4 and BKCa for treatment of brain diseases. Bioorganic & Medicinal Chemistry. 2020; 28: 115609. https://doi.org/10.1016/j.bmc.2020.115609.

[14] Kanju P, Liedtke W. Pleiotropic function of TRPV4 ion channels in the central nervous system. Experimental Physiology. 2016; 101: 1472–1476. https://doi.org/10.1113/EP085790.

[15] Bai JZ, Lipski J. Involvement of TRPV4 channels in Aβ(40)-induced hippocampal cell death and astrocytic Ca(2+) signalling. Neurotoxicology. 2014; 41: 64–72. https://doi.org/10.1016/j.neuro.2014.01.001.

[16] Zhang L, Papadopoulos P, Hamel E. Endothelial TRPV4 channels mediate dilation of cerebral arteries: impairment and recovery in cerebrovascular pathologies related to Alzheimer's disease. British Journal of Pharmacology. 2013; 170: 661–670. https://doi.org/10.1111/bph.12315.

[17] Lee JC, Choe SY. Age-related changes in the distribution of transient receptor potential vanilloid 4 channel (TRPV4) in the central nervous system of rats. Journal of Molecular Histology. 2014; 45: 497–505. https://doi.org/10.1007/s10735-014-9578-z.

[18] Dai XJ, Li N, Yu L, Chen ZY, Hua R, Qin X, *et al*. Activation of BV2 microglia by lipopolysaccharide triggers an inflammatory reaction in PC12 cell apoptosis through a toll-like receptor 4-dependent pathway. Cell Stress & Chaperones. 2015; 20: 321–331. https://doi.org/10.1007/s12192-014-0552-1.

[19] Fukuda N, Toriuchi K, Mimoto R, Aoki H, Kakita H, Suzuki Y, *et al*. Hypothermia Attenuates Neurotoxic Microglial Activation via TRPV4. Neurochemical Research. 2024; 49: 800–813. https://doi.org/10.1007/s11064-023-04075-8.

[20] Redmon SN, Yarishkin O, Lakk M, Jo A, Mustafić E, Tvrdik P, *et al*. TRPV4 channels mediate the mechanoresponse in retinal

microglia. Glia. 2021; 69: 1563–1582. https://doi.org/10.1002/glia.23979.

[21] da Silva RA, Roda VMDP, Akamine PS, da Silva DS, Siqueira PV, Matsuda M, *et al*. Blockade of the TGF-β pathway by galunisertib inhibits the glial-mesenchymal transition in Müller glial cells. Experimental Eye Research. 2023; 226: 109336. https://doi.org/10.1016/j.exer.2022.109336.

[22] Liu Y, Dai Y, Li Q, Chen C, Chen H, Song Y, *et al*. Beta-amyloid activates NLRP3 inflammasome via TLR4 in mouse microglia. Neuroscience Letters. 2020; 736: 135279. https://doi.org/10.1016/j.neulet.2020.135279.

[23] Lindner B, Burkard T, Schuler M. Phagocytosis assays with different pH-sensitive fluorescent particles and various readouts. BioTechniques. 2020; 68: 245–250. https://doi.org/10.2144/btn-2020-0003.

[24] Peng S, Poole DP, Veldhuis NA. Mini-review: Dissecting receptor-mediated stimulation of TRPV4 in nociceptive and inflammatory pathways. Neuroscience Letters. 2022; 770: 136377. https://doi.org/10.1016/j.neulet.2021.136377.

[25] Chen Y, Yu Y. Tau and neuroinflammation in Alzheimer's disease: interplay mechanisms and clinical translation. Journal of Neuroinflammation. 2023; 20: 165. https://doi.org/10.1186/s12974-023-02853-3.

[26] Bai J, Geng B, Wang X, Wang S, Yi Q, Tang Y, *et al*. Exercise Facilitates the M1-to-M2 Polarization of Microglia by Enhancing Autophagy via the BDNF/AKT/mTOR Pathway in Neuropathic Pain. Pain Physician. 2022; 25: E1137–E1151.

[27] Si W, Li X, Jing B, Chang S, Zheng Y, Chen Z, *et al*. Stigmasterol regulates microglial M1/M2 polarization via the TLR4/NF-κB pathway to alleviate neuropathic pain. Phytotherapy Research: PTR. 2024; 38: 265–279. https://doi.org/10.1002/ptr.8039.

[28] Mitchell K, Shah JP, Tsytsikova LV, Campbell AM, Affram K, Symes AJ. LPS antagonism of TGF-β signaling results in prolonged survival and activation of rat primary microglia. Journal of Neurochemistry. 2014; 129: 155–168. https://doi.org/10.1111/jnc.12612.

[29] Ogunrinade FA, Iwuanyanwu VU, Sarker SD, Olajide OA. Neuroprotection by Skimmianine in Lipopolysaccharide-Activated BV-2 Microglia. Molecules (Basel, Switzerland). 2023; 28: 1317. https://doi.org/10.3390/molecules28031317.

[30] Elmazoglu Z, Kayhan H, Santamaría A, Rangel-López E, Uğur PK, Ceylan A, *et al*. Platinum nanoparticles Protect Against Lipopolysaccharide-Induced Inflammation in Microglial BV-2 Cells via Decreased Oxidative Damage and Increased Phagocytosis. Neurochemical Research. 2021; 46: 3325–3341. https://doi.org/10.1007/s11064-021-03434-7.

[31] Song Y, Zhan L, Yu M, Huang C, Meng X, Ma T, *et al*. TRPV4 channel inhibits TGF-β1-induced proliferation of hepatic stellate cells. PloS One. 2014; 9: e101179. https://doi.org/10.1371/journal.pone.0101179.

[32] Garcia-Elias A, Mrkonjić S, Jung C, Pardo-Pastor C, Vicente R, Valverde MA. The TRPV4 channel. Handbook of Experimental Pharmacology. 2014; 222: 293–319. https://doi.org/10.1007/978-3-642-54215-2_12.

[33] Tang Y, Le W. Differential Roles of M1 and M2 Microglia in Neurodegenerative Diseases. Molecular Neurobiology. 2016; 53: 1181–1194. https://doi.org/10.1007/s12035-014-9070-5.

[34] Ren X, Gao X, Li Z, Ding Y, Xu A, Du L, *et al*. Electroacupuncture ameliorates neuroinflammation by inhibiting TRPV4 channel in ischemic stroke. CNS Neuroscience & Therapeutics. 2024; 30: e14618. https://doi.org/10.1111/cns.14618.

[35] Liu X, Cai H, Peng L, Ma H, Yan Y, Li W, *et al*. Microglial Nrf2/HO-1 signaling gates remifentanil-induced hyperalgesia via suppressing TRPV4-mediated M1 polarization. Free Radical Biology & Medicine. 2024; 214: 87–100. https://doi.org/10.1016/j.freeradbiomed.2024.01.047.

[36] Capece D, Verzella D, Flati I, Arboretto P, Cornice J, Franzoso G. NF-κB: blending metabolism, immunity, and inflammation. Trends in Immunology. 2022; 43: 757–775. https://doi.org/10.1016/j.it.2022.07.004.

[37] Sun E, Motolani A, Campos L, Lu T. The Pivotal Role of NF-kB in the Pathogenesis and Therapeutics of Alzheimer's Disease. International Journal of Molecular Sciences. 2022; 23: 8972. https://doi.org/10.3390/ijms23168972.

[38] Xie Y, Chen X, Li Y, Chen S, Liu S, Yu Z, *et al*. Transforming growth factor-β1 protects against LPC-induced cognitive deficit by attenuating pyroptosis of microglia via NF-κB/ERK1/2 pathways. Journal of Neuroinflammation. 2022; 19: 194. https://doi.org/10.1186/s12974-022-02557-0.

[39] Wang Y, Jin Z, Jia S, Shen P, Yang Y, Huang Y. Mechanical stress protects against chondrocyte pyroptosis through TGF-β1-mediated activation of Smad2/3 and inhibition of the NF-κB signaling pathway in an osteoarthritis model. Biomedicine & Pharmacotherapy = Biomedecine & Pharmacotherapie. 2023; 159: 114216. https://doi.org/10.1016/j.biopha.2023.114216.

[40] Srivastava S, Ahmad R, Khare SK. Alzheimer's disease and its treatment by different approaches: A review. European Journal of Medicinal Chemistry. 2021; 216: 113320. https://doi.org/10.1016/j.ejmech.2021.113320.